

FLC FOR ELECTRIC VEHICLE APPLICATIONS IN POWER OPTIMISATION SCHEME OF INDUCTION MOTOR

1ANURAG KOMIRI, 2DR. P. DURAI PANDY

1MTEch Student, 2MTEch. Ph.D. Associate Professor, HOD

J.B. INSTITUTE OF ENGINEERING & TECHNOLOGY, Hyderabad, INDIA

Abstract: Energy efficiency is crucial in electric cars (EVs) and hybrid EVs since the energy storage is constrained. The induction motor efficiency increases with loss minimization, which is in addition to its excellent stability and inexpensive cost. Also, while it is functioning at less than full load, it may use more energy than is really required to carry out its functions. This paper suggests a fuzzy logic control (FLC)-based control approach for use in electric vehicle applications. The initial current amplitude may be increased using FLC controller, and more electricity is saved. Simulation was used to confirm the effectiveness of this control using the MATLAB/SIMULINK software suite. The simulation techniques provide excellent, high-performance outcomes in time-domain response and swift rejection of system-affected disturbance when compared to the standard proportional integral derivative controller. As a result, the induction motor's core losses are drastically decreased, which raises the drive system's efficiency. The experimental findings from the authors' laboratory, which are in excellent accord with the outcomes of the simulation, justify the recommended control system.

1 Introduction

Particularly in the previous several decades, the heavy use of fossil fuels has increased dramatically, which has increased the atmospheric CO₂ concentration. Global initiatives to decrease carbon dioxide are now urgently needed as concerns about climate change and increasing sea levels brought on by global warming become more severe. Vehicle fuel economy must be significantly increased since transportation accounts for 20% of all carbon dioxide emissions [1-6]. Since they are more effective, ecologically friendly, quiet, and often less energy dependent, electric vehicles (EVs) provide a number of benefits [7]. The effectiveness and cost of the drive are significantly impacted by the choice of the electric machine. Yet any drive, even those that may be incorporated into EVs and hybrid EVs, must have electric machinery [8]. The two major machine types that may be used in EVs are synchronous motors and induction motors (IMs) [9]. .. and.....

Because of its strength, cheap cost, and little maintenance requirements, the IM is increasingly often used for traction drives and is the ideal choice for EVs [13–16]. Nevertheless, due of its greater losses in the EV application [17–18], the machine efficiency suffers. Low

energy density, larger weight, longer charging periods, and longer battery life are the main constraining factors to integrating such cars into the transportation system [19]. As a result, EV functioning depends on the best possible usage of energy [2022]. It is commonly accepted that proportional integral derivative (PID) control, which is used in many industrial drives, is one of the most prevalent units due to its efficacy and ease of implementation. PID controllers are also employed in industrial applications and are a component of the majority of current control loops [23, 24]. Due to component obsolescence or a change in the working environment, considerable performance loss may happen when the operating circumstances are changed [25]. Fuzzy logic control (FLC), for example, is an intelligent control approach that may be used to deliver superior performance due to the uncertainty and complexity of modelling the accurate analytical model of a controlled system [26–28]. Several strategy rules in the FLC framework make simpler use of linguistic tags. Other other EV energy demand management projects have followed this strategy [7]. A mathematical model of a controlled system is not necessary for FLC since it is a model-free technique [28, 29]. Thus, the FLC system controller should be created with adaptive features when the system reaches regions with

and underwater vessels, electric aircraft and electric spacecraft.

EVs first came into existence in the mid-19th century, when electricity was among the preferred methods for motor vehicle propulsion, providing a level of comfort and ease of operation that could not be achieved by the gasoline cars of the time. Modern internal combustion engines have been the dominant propulsion method for motor vehicles for almost 100 years, but electric power has remained commonplace in other vehicle types, such as trains and smaller vehicles of all types.

In the 21st century, EVs saw a resurgence due to technological developments, and an increased focus on renewable energy. A great deal of demand for electric vehicles developed and a small core of do-it-yourself (DIY) engineers began sharing technical details for doing electric vehicle conversions. Government incentives to increase adoptions were introduced, including in the United States and the European Union

MULTI LEVEL INVERTER

An inverter is an electrical device that converts direct current (DC) to alternating current (AC) the converted AC

can be at any required voltage and frequency with the use of appropriate transformers, switching, and control circuits. Static inverters have no moving parts and are used in a wide range of applications, from small switching power supplies in computers, to large electric utility high voltage direct current applications that transport bulk power. Inverters are commonly used to supply AC power from DC sources such as solar panels or batteries. The electrical inverter is a high power electronic oscillator. It is so named because early mechanical AC to DC converters were made to work in reverse, and thus were "inverted", to convert DC to AC.

4.1 Cascaded H-Bridges inverter

A single phase structure of an m-level cascaded inverter is illustrated in Figure 4.1. Each separate DC source (SDCS) is connected to a single phase full bridge, or H-bridge, inverter. Each inverter level can generate three different voltage outputs, $+V_{dc}$, 0, and $-V_{dc}$ by connecting the DC source to the ac output by different combinations of the four switches, S_1 , S_2 , S_3 , and S_4 . To obtain $+V_{dc}$, switches S_1 and S_4 are turned on, whereas $-V_{dc}$ can be obtained by turning on switches S_2 and S_3 . By turning on S_1 and S_2 or S_3 and S_4 , the output voltage

is 0. The AC outputs of each of the different full bridge inverter levels are connected in series such that the synthesized voltage waveform is the sum of the inverter outputs. The number of output phase voltage levels m in a cascade inverter is defined by $m = 2s+1$, where s is the number of separate DC sources. An example phase voltage waveform for an 11 level cascaded H-bridge inverter with 5 SDCSs and 5 full bridges is shown in Figure 4.2. The phase voltage

$$V_{an} = V_{a1} + V_{a2} + V_{a3} + V_{a4} + V_{a5} \dots(4.1)$$

For a stepped waveform such as the one depicted in Figure 4.2 with s steps, the Fourier Transform for this waveform follows

$$V(\omega t) = \frac{4V_{dc}}{\pi} \sum_n [\cos(n\theta_1) + \cos(n\theta_2) + \dots + \cos(n\theta_s)] \frac{\sin(n\omega t)}{n}, \text{ where } n = 1,3,5,7 \dots \dots(4.2)$$

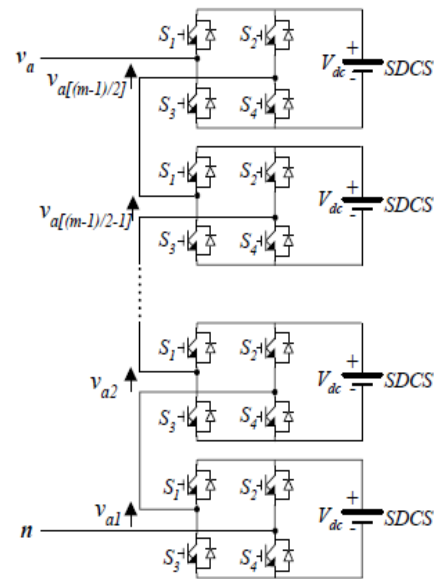


Fig.4.1Single-phase structure of a multilevel cascaded H-bridges inverter

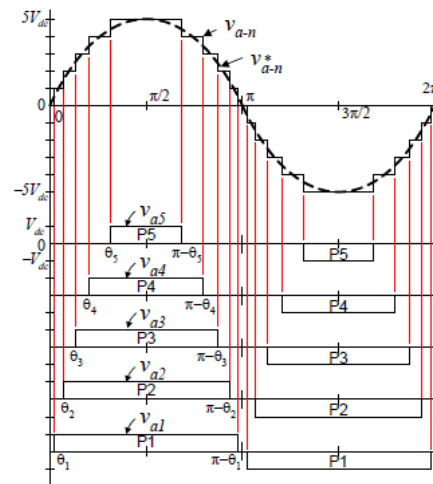


Fig.4.2 Output phase voltage waveform of an 11 level cascade inverter with 5 separate dc sources.

Introduction to fuzzy

In recent years, the number and variety of applications of fuzzy logic have increased significantly. The applications range from consumer products such as cameras, camcorders, washing machines, and microwave ovens to industrial process control, medical instrumentation, decision support systems, and portfolio selection. To understand why use of fuzzy logic has grown, you must first understand what is meant by fuzzy logic.

Fuzzy logic has two different meanings. In a narrow sense, fuzzy logic is a logical system, which is an extension of multivalve logic. However, in a wider sense fuzzy logic (FL) is almost synonymous with the theory of fuzzy sets, a theory which relates to classes of objects with un sharp boundaries in which membership is a matter of degree. In this perspective, fuzzy logic in its narrow sense is a branch of FL. Even in its more narrow definition, fuzzy logic differs both in concept and substance from traditional multivalve logical systems.

6.2 What is fuzzy logic?

Fuzzy logic is all about the relative importance of precision is how important is

it to be exactly right when a rough answer will do?

You can use Fuzzy Logic Toolbox software with MATLAB technical computing software as a tool for solving problems with fuzzy logic. Fuzzy logic is a fascinating area of research because it does a good job of trading off between significance and precision something that humans have been managing for a very long time. In this sense, fuzzy logic is both old and new because, although the modern and methodical science of fuzzy logic is still young, the concept of fuzzy logic relies on age old skills of human reasoning.

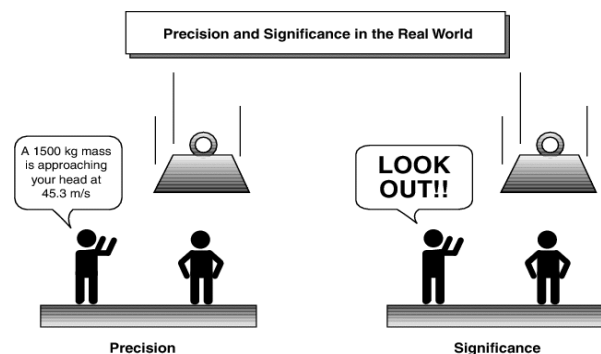


Fig.6.1 Fuzzy descriptions

Speed control using FLC

Two input variables for FLC in the case of motor speed control are needed, which are the motor speed error (w_e) and its derivative that represents the speed variation error (Δw_e). Speed error and speed variation error could be described as follows:

$$w_e = w_{ref}^* - w_{act} \quad (6)$$

where w^*_{ref} and w_{act} denote the reference motor speed and the actual/or measured motor speed, respectively:

$$\frac{dw_e}{dt} = \frac{\Delta w_e}{T_s} \tag{7}$$

The controller output is the incremental change of the control signal Δu . The control signal can be obtained by

$$\Delta u = \Delta t_e^* = k_1 \cdot w_e + k_2 \cdot \Delta w_e \tag{8}$$

where k_1 and k_2 represent the current and previous states of the system, respectively. The universe of discourse in all membership functions of the controller inputs, i.e., w_e and Δw_e , and the output, i.e. Δu , are defined on the normalised domain $[-1, 1]$, as shown in Fig. 5.

Five membership function (MF) for inputs and five MF for output fuzzy sets have been used to partition the fuzzy logic membership functions as shown in Fig. 5.

To relate two input variables to one output variable, a Mamdani fuzzy inference system is used in this system. The two input variables are the error (w_e), which are the differences between the desired (set-point) and measured speed, and the change of error (Δw_e). The scaling factors G_e , G_{de} , and G_u , in Fig. 4, which perform the normalisation process and denormalisation of the specific variables of a conventional control gain. When G_e , G_{de} , and G_u are the error measurement, error variation, and FLC output factors respectively, the value of these measurement factors is based on the initial error. Limited models are used to reduce the error and variation in the error between (1, -1) the input and output functions of the FLC as shown in Fig. 5, while the FLC rules are

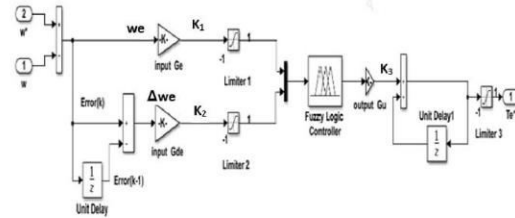


Fig. 4 Detailed construction of the fuzzy controller

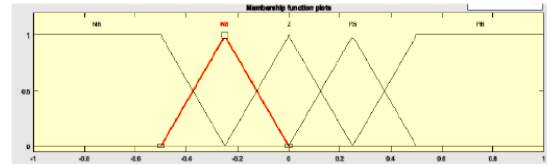


Fig. 5 Membership function of FLC (w_e), (Δw_e), (Δu)

Table 1 Rules of the FLC

Δw_e	w_e				
	NB	NS	Z	PS	PB
NB	NB	NB	NS	NS	Z
NS	NB	NS	NS	Z	PS
Z	NS	NS	Z	PS	PS
PS	NS	Z	PS	PS	PB
PB	Z	PS	PS	PB	PB

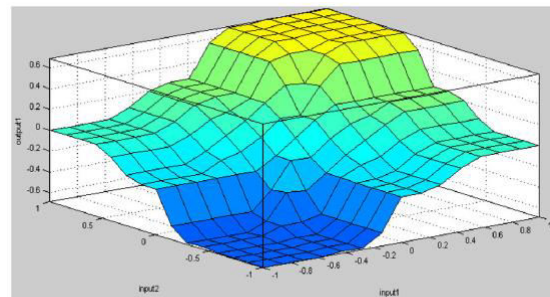


Fig. 6 Crisp in./out. map

registered in Table 1. This feature gives a hint of using the interpolation of the basic table of rules to create a more precise continuous control rule than simply taking NB, NS, Z, PS, and PB stand for negative big, negative small, zero, positive small, and positive big, respectively. Here except for two obscure groups at the outer ends (trapezoidal MFs are chosen), symmetrical triangles are selected with an equal base and 50% overlap with adjacent MFs.

As shown in Table 1, there are five fuzzy subsets for each variable, which gives 25 possible rules, where the typical rule is: ‘If e is NB and de is PB Then u is Z’.

Speed correction control is a need because the motor speed and output power are altered by the perturbation approach. The motor's output rotor speed should be maintained as constant as possible. The input/output mapping of the FLC is shown in Fig. 6.

Smooth torque and improvement in the system performance can be produced for EV applications by using this fuzzy controller in the outer loop by taking the speed error and variation of error as input signals to create the equivalent control terms.

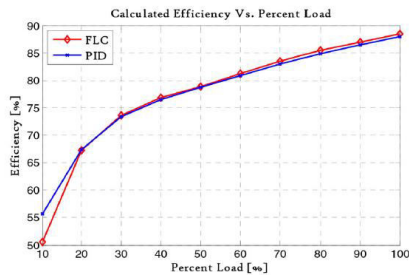


Fig. 7 Efficiency of the IM drive using PID versus FLC

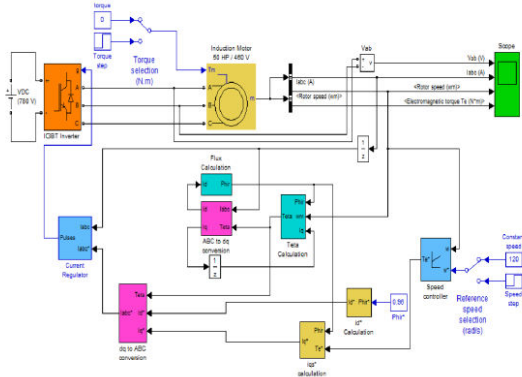


Fig. 8 MATLAB model of three-phase IM

PROJECT DESCRIPTION AND CONTROL DESIGN CIRCUIT DESCRIPTION

As shown in Fig. 1, battery EV is electrically operated vehicle alone and consists of three main parts: firstly, an electric motor system, often there is only one electrical machine, usually, a three-phase AC. Connected to the wheel via the gearbox and differential. Secondly, a battery that acts

as a power store, and the energy is stored chemically in the battery, which is plugged into the device by an electronic DC/AC power adapter accompanied by the control system. Lastly, the three-phase frequency and voltage control system applied to the electric machine, depending on the current driver's request, which is connected by the accelerator pedal and/or brake pedal.

In Fig. 1 the three-phase electric machine provides traction power for wheels. The differential with gear ratio for high-speed adjustment of the electric motor shaft to the low speed of the wheels will provide torque for the left and right wheels. The speed of the machine is controlled by an inverter that converts the battery voltage DC to the three-phase AC voltage. It is important to include losses from components when analysing the power consumption of an EV that is not part of the power chain from the grid to the wheels. To push the EV system into the required operation, our commitment is to create suitable controllers for feedback. The inadequately adaptable, flexible and powerful controller can be implemented by adopting FLC techniques for EVs applications.

CONTROL PRINCIPLE Conventional PID control

A classical PID controller is introduced in the first design approach for applying to an indirect field-oriented IM order to control its speed and also starting situation is investigated. As illustrated in Fig. 2 the proposed control system includes a (direct-quadrature-zero) conversion equations, and a phase-locked loop algorithm that synchronises with the utility current regulator. The phase currents (i_a, i_b, i_c) are converted from a-b-c coordinates to a d-q frame. The components of d-q can be described using the following conversions:

$$\begin{bmatrix} i_d \\ i_q \end{bmatrix} = \sqrt{\frac{2}{3}} \begin{bmatrix} \sin(\omega t) & \sin(\omega t - \frac{2\pi}{3}) & \sin(\omega t + \frac{2\pi}{3}) \\ \cos(\omega t) & \cos(\omega t - \frac{2\pi}{3}) & \cos(\omega t + \frac{2\pi}{3}) \end{bmatrix} \times \begin{bmatrix} i_{sa} \\ i_{sb} \\ i_{sc} \end{bmatrix} \quad (1)$$

The active and reactive power calculated now includes oscillation and average components. However, two outer PID control loops are utilised to acquire the average components to the outputs of the active power and reactive power. A block diagram of the conventional PID control is given in Fig. 3. This PID produces active current reference (id*) and reactive current reference (iq*), as given in the following conversions:

$$i_d^* = k_p(P_{ref} - P) + k_i \int (P_{ref} - P) dt \quad (2)$$

$$i_q^* = k_p(Q_{ref} - Q) + k_i \int (Q_{ref} - Q) dt \quad (3)$$

where kp is the proportional constant and ki is the basic constant, for the PID controllers used. Pref is the charging power reference and Qref is the reference value of the reactive power required by the AC source.

The control is designed by integrating the inner current loop and the outer voltage loop. When comparing the current reference with the actual current in the outer loop produces the current reference, and it is used to control the inner loop. Consequently, the internal PID loops are generated by comparing the measured line currents obtained using the Park conversion. The results (ed and eq) are first summarised by the disengagement conditions and then normalised by the DC voltage to obtain the operating ratios in the d–q coordinates as follows:

$$\begin{bmatrix} d_d \\ d_q \end{bmatrix} = \frac{1}{V_{dc}} \begin{bmatrix} e_d + v_d + 3\omega L \times i_q \\ e_q + v_q - 3\omega L \times i_d \end{bmatrix} \quad (4)$$

Inverse matrix transformation can be used to obtain the duty ratios in (a–b–c) frame coordinates, which can be expressed as follows:

$$\begin{bmatrix} D_a \\ D_b \\ D_c \end{bmatrix} = \sqrt{\frac{2}{3}} \begin{bmatrix} \sin(\omega t) & \cos(\omega t) \\ \sin(\omega t - \frac{2\pi}{3}) & \cos(\omega t - \frac{2\pi}{3}) \\ \sin(\omega t + \frac{2\pi}{3}) & \cos(\omega t + \frac{2\pi}{3}) \end{bmatrix} \times \begin{bmatrix} d_d \\ d_q \end{bmatrix} \quad (5)$$

Description of suggested FLC

Due to the non-linear characteristics of AC motors, especially the squirrel cage induction motor (SCIM), controlling this problem remains a difficult problem because many factors (mainly rotor resistances) vary with operating conditions. Therefore, traditional control technology (PID) must be changed using the effective intelligent FLC [37] for EV applications. The most important considerations in the design of any fuzzy system are:

- (i) generation of fuzzy rules for some control issues, which are created by experts in the area;
- (ii) selecting the membership functions and adjusting;
- (iii) selecting the scaling factors.

In the second design approach, the basic FLC was developed for EV applications, which serve as a type of variable structure control unit that is well established for stability and durability. Fig. 4 shows a typical FLC.

A new approach to improve adjustable speed drives voltage, frequency, and current control is provided using the mathematical technique called fuzzy logic. It can be applied to problems that make non-linearity and its dynamic nature intractable by conventional control methods in for EV applications. Motor control has all the characteristics of this type of problem.

Power loss calculations and efficiency of induction motor drive

The following power losses of the proposed control scheme at full load for a worst-case scenario are estimated to verify the measured efficiency.

4.1 Parameters

This section shows the entire given and calculated parameters in Table 2. The

parameters come from the typical values listed in the datasheets. Next, some calculated parameters will be shown, and the stray losses are negligible in [38].

4.2 Input power losses

Three-phase IM is drawing 62.6 A at 0.85 PF lagging using PID, and 60 A at 0.85 PF lagging using FLC. The input power losses can be estimated as

$$P_{In} = \sqrt{3} \times V_L I_L \cos \theta = 3 \times V_{ph} I_{ph} \cos \theta \tag{9}$$

4.3 Air-gap power losses

The stator copper losses are 2 kW, and the core losses are 1.8 kW, which is taken into consideration. The air-gap power losses can be estimated as

$$P_{AG} = P_{In} - (P_{SCL} + P_{Core}) = P_{Conv} + P_{RCL} = 3I_2^2 \frac{R_2}{S} = \frac{P_{RCL}}{S} \tag{10}$$

Table 2 Given and calculated parameters

Item	Symbol	Value
voltage (line-to-line)	V_L	460 V
frequency	F	60 Hz
number of poles	P	4
power factor	PF	0.85 lagging
three-phase IM is drawing (PID)	I_L	62.6 A
three-phase IM is drawing (FLC)	I_L	60 A
stator copper losses (PID)	P_{SCL}	2 kW
stator copper losses (FLC)	P_{SCL}	1.8 kW
rotor copper losses (PID)	P_{RCL}	700 W
rotor copper losses (FLC)	P_{RCL}	500 W
core losses	P_{Core}	1.8 kW
friction and windage losses	$P_{F\&W}$	600 W

Table 3 Results of power losses analysis under full load and efficiency estimation of IM drive using PID and FLC

Item	Power losses calculation	PID	FLC
input power	$P_{In} = \sqrt{3} \times V_L I_L \cos \theta = 3 \times V_{ph} I_{ph} \cos \theta$	42.395 kW	40.634 kW
air-gap power losses	$P_{AG} = P_{In} - (P_{SCL} + P_{Core})$	38.595 kW	37.034 kW
converted power losses	$P_{Conv} = P_{AG} - P_{RCL}$	37.895 kW	36.534 kW
output power	$P_{out} = P_{Conv} - (P_{f\&w} + P_{stray})$	37.295 kW	35.934 kW
efficiency	$\eta = \frac{P_{out}}{P_{in}} \times 100$	87.97%	88.43%

4.4 Converted power losses

To calculated power converted, the only rotor copper losses are 700 W, is that taken into consideration. The converted power losses can be estimated as

$$P_{Conv} = P_{AG} - P_{RCL} = 3I_2^2 \frac{R_2(1-S)}{S} = \frac{P_{RCL}(1-S)}{S} \tag{11}$$

$$P_{Conv} = (1-S)P_{AG} \tag{12}$$

4.5 Output power losses

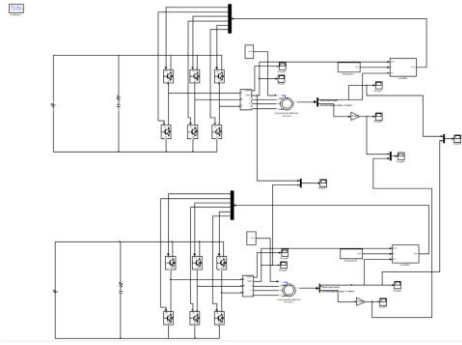
The calculation assumes that stray losses are negligible and thus the friction and windage losses are 600 W, which is that taken into respect. The output power losses can be estimated as shown in Table 3

$$P_{Out} = P_{Conv} - (P_{f+w} + P_{stray}) \tag{13}$$

From this figure, the energy efficiency increases when the IM runs at optimal performance. By comparison between the results obtained by the controller tuned using some known tuning rules and the results obtained by the suggested rules, a worthier performance is achieved by the proposed.

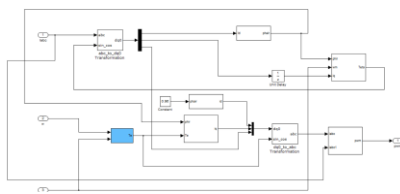
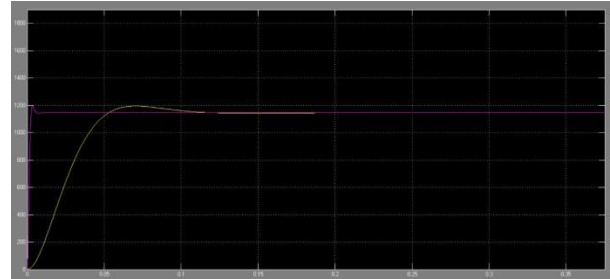
Simulation results

Simulink and power sum toolboxes of MATLAB software are used in the simulation, where two cases have been considered as shown in Fig. 8. In the first case study, a 50 hp IM is powered using a PID controller. Three-phase voltage and current are measured and planned in the first 5 s of operation. Also, the probe is made in the acceleration curve and the resulting torque. In the second case, the motor itself is operated using FLC. PID controller response is compared with the FLC response and the results are shown in Figs. 9–11.



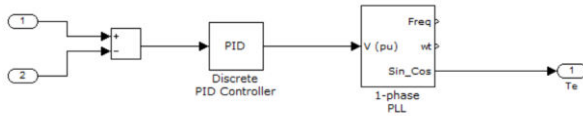
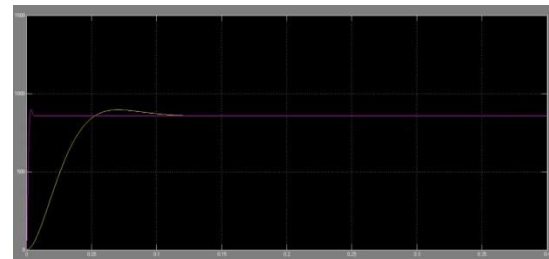
SIMULATION CIRCUIT CONFIGURATION

Fig. 14 Speed response comparison for PID and FLC when the reference speed is 1432 rpm



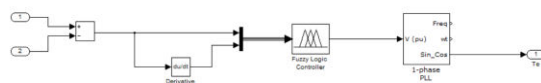
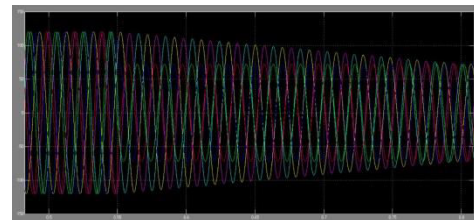
PROPOSED CONTROL CIRCUIT

Fig. 15 Speed response comparison for PID and FLC when the reference speed is 1145 rpm



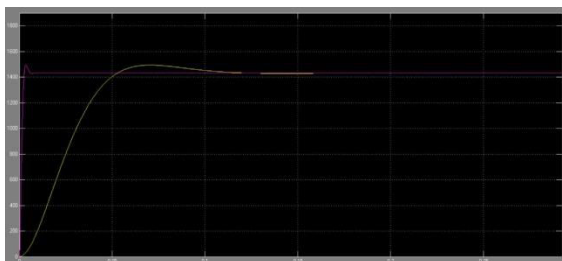
Block diagram of the conventional PID controller

Fig. 16 Speed response comparison for PID and FLC when the reference speed is 859 rpm



Block diagram of the conventional FUZZY controller

Fig. 9 Three-phase stator current of PID and FLC models (A)



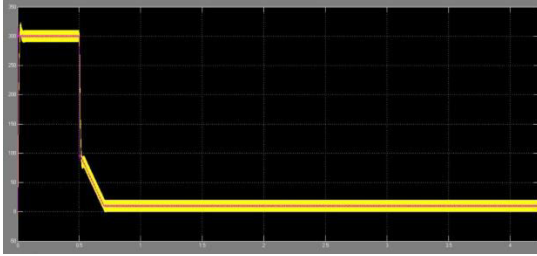
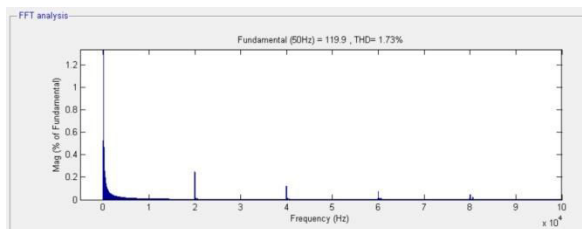
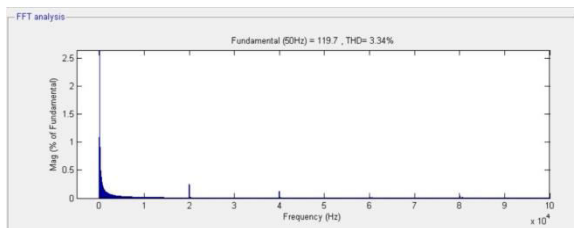


Fig. 11 Simulation response of PID and FLC for electromagnetic torque

(N m)



harmonics in FUZZY mode



harmonics in PID mode

CONCLUSION

IM may use more power than necessary if it is operating at less than full load. Heat is the result of this extra power. More power may be conserved during this period by utilising the FLC to adjust the initial current amplitude. The speed error and change of error are the inputs to the fuzzy controller, which are employed in the outer loop to create an equivalent controller term. In this work, a simulation analysis using a 50 hp IM-driven EV was carried out. Tests are conducted on a variety of performance measures, including peak

overshoot, steady-state error, rising time, and settling time. The findings demonstrated that the recommended system's phase current had less loss (reduced amplitude) while maintaining the same order components. For the real torque in the steady state, the loss amplitudes are often minimised. It accomplishes smooth torque and raises system efficiency. The simulation results of the proposed FLC scheme demonstrated extremely strong stability and superior performance in terms of rising time, settling time, and peak overshoot compared to the traditional PID controller. The experimental findings, which are in excellent agreement with the modelling results, support the suggested control system.

References

- [1] Sato, E.: 'Permanent magnet synchronous motor drives for hybrid electric vehicles', *IEEJ Trans. Electr. Electron. Eng.*, 2007, 2, (2), pp. 162–168
- [2] Agency, I.E.: 'Global EV outlook 2016: beyond one million electric cars' (OECD Publishing)
- [3] Sayed, K.: 'Zero-voltage soft-switching DC-DC converter-based charger for LV battery in hybrid electric vehicles', *IET Power Electron.*, 2019, 12, (13), pp. 3389–3396
- [4] Gomez, J.C., Morcos, M.M.: 'Impact of EV battery chargers on the power quality of distribution systems', *IEEE Power Eng. Rev.*, 2002, 22, (10), pp. 63–63
- [5] Stephan, C.H., Sullivan, J.: 'Environmental and energy implications of plugin hybrid-electric vehicles', *Environ. Sci. Technol.*, 2008, 42, (4), pp. 1185–1190
- [6] Umetani, S., Fukushima, Y., Morita, H.: 'A linear programming based heuristic algorithm for charge and discharge scheduling of electric vehicles in a building energy management system', *Omega*, 2017, 67, pp. 115–122

- [7] Trovao, J.P.F., Roux, M.-A., Menard, E., et al.: 'Energy and power-split management of dual energy storage system for a three-wheel electric vehicle', *IEEE Trans. Veh. Technol.*, 2017, 66, (7), pp. 5540–5550
- [8] Buyukdegirmenci, V.T., Bazzi, A.M., Krein, P.T.: 'Evaluation of induction and permanent-magnet synchronous machines using drive-cycle energy and loss minimization in traction applications', *IEEE Trans. Ind. Appl.*, 2014, 50, (1), pp. 395–403
- [9] Sarigiannidis, A.G., Beniakar, M.E., Kladas, A.G.: 'Fast adaptive evolutionary PM traction motor optimization based on electric vehicle drive cycle', *IEEE Trans. Veh. Technol.*, 2016, 66, (7), pp. 5762–5774
- [10] Wang, Q., Niu, S., Luo, X.: 'A novel hybrid dual-PM machine excited by AC with DC bias for electric vehicle propulsion', *IEEE Trans. Ind. Electron.*, 2017, 64, (9), pp. 6908–6919
- [11] Boukadida, S., Gdaim, S., Mtiba, A.: 'Sensor fault detection and isolation based on artificial neural networks and fuzzy logic applied on induction motor for electrical vehicle', *Int. J. Power Electron. Drive Syst.*, 2017, 8, (2), pp. 601–611
- [12] Varghese, S.T., Rajagopal, K.R.: 'Economic and efficient induction motor controller for electric vehicle using improved scalar algorithm'. *IEEE 1st Int. Conf. on Power Electronics, Intelligent Control and Energy Systems (ICPEICES)*, Delhi, 2016, pp. 1–7
- [13] Ulu, C., Korman, O., Komurgoz, G.: 'Electromagnetic and thermal analysis/design of an induction motor for electric vehicles'. *The 8th Int. Conf. on Mechanical and Aerospace Engineering (ICMAE)*, Prague, 2017, pp. 6–10
- [14] Ouchatti, A., Abbou, A., Akherraz, M., et al.: 'Sensorless direct torque control of induction motor using fuzzy logic controller applied to electric vehicle'. *Int. Renewable and Sustainable Energy Conf. (IRSEC)*, Ouarzazate, 2014, pp. 366–372
- [15] Makrygiorgou, J.J., Alexandridis, A.T.: 'Induction machine driven electric vehicles based on fuzzy logic controllers'. *The 42nd Annual Conf. of the IEEE Industrial Electronics Society*, Florence, 2016, pp. 184–189
- [16] Li, H., Klontz, K.W.: 'Rotor design to reduce secondary winding harmonic loss for induction motor in hybrid electric vehicle application'. *IEEE Energy Conversion Congress and Exposition (ECCE)*, Milwaukee, WI, 2016, pp. 1–6
- [17] Kumar, R., Das, S., Chattopadhyay, A.K.: 'Comparative assessment of two different model reference adaptive system schemes for speed-sensorless control of induction motor drives', *IET Electr. Power Appl.*, 2016, 10, (2), pp. 141–154
- [18] Saleeb, H., Sayed, K., Kassem, A., et al.: 'Power management strategy for battery electric vehicles', *IET Electr. Syst. Transp.*, 2019, 9, (2), pp. 65–74
- [19] Das, S., Pal, A., Manohar, M.: 'Adaptive quadratic interpolation for loss minimization of direct torque controlled induction motor driven electric vehicle'. *IEEE 15th Int. Conf. on Industrial Informatics (INDIN)*, Emden, 2017, pp. 641–646